ChemComm

CrossMark
← click for updates

Discrete polygonal supramolecular architectures of isocytosine-based Pt(II) complexes at the solution/graphite interface†

Mohamed El Garah,[a] Stephan Sinn,[b] Arezoo Dianat,[c] Alejandro Santana-Bonilla,[c] Rafael Gutierrez,[c] Luisa De Cola,[b] Gianaurelio Cuniberti,*[cde] Artur Ciesielski[a] and Paolo Samorì*[a]

Polygonal supramolecular architectures of a Pt(II) complex including trimers, tetramers, pentamers and hexamers were self-assembled *via* hydrogen bonding between isocytosine moieties; their structure at the solid/liquid interface was unravelled by *in situ* scanning tunneling microscopy imaging. Density functional theory calculations provided in-depth insight into the thermodynamics of their formation by exploring the different energy contributions attributed to the molecular self-assembly and adsorption processes.
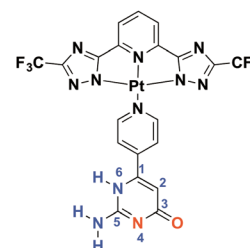
Molecular self-assembly at surfaces is a versatile approach to position functional groups with sub-nanometer precision over several hundreds of µm² areas and thereby it allows the fine-tuning of numerous physico-chemical properties of the resulting nanostructures.[1–6] The design of molecules comprising active groups represents a promising route for engineering functional surfaces and interfaces. Among various functional systems, luminescent Pt(II) complexes have attracted great interest during the last decade due to their appealing photophysical and redox properties, including strong absorption bands featuring onsets in the visible region as well as room temperature emission accompanied by a large Stokes shift.[7] Neutral Pt(II) complexes bearing tridentate azolate-based ligands possess extraordinarily high phosphorescence quantum yields and long excited state life-times.[8,9] Furthermore, due to their square-planar geometry such complexes display high propensity to undergo aggregation by means of the solvophobic effects, π–π and dispersive interactions.

These properties can lead to supramolecular assemblies holding attractive features, because closed-shell metal–metal interactions of the Pt(II) centers strongly augment the emission properties.[10–13]

Scanning tunnelling microscopy (STM) is an extremely powerful tool to investigate supramolecular materials featuring atomic resolution. In particular, it is the method of choice for imaging structures and dynamics in molecular self-assembly on surfaces.[14–18]

Hydrogen bonding has been extensively used as a directional, non-covalent intermolecular interaction for designing and controlling the formation of complex supramolecular architectures. On solid surfaces, sophisticated structures can result from the formation of various hydrogen bonded patterns, including linear and cyclic motifs with different pairings such as O–H···O, N–H···O and N–H···N.[19–23] Nucleobases have been previously reported to form cyclic quartet structures on the surface[23–26] and pentamers in the solution.[27] To the best of our knowledge, the formation of other types of cyclic motifs has not been discussed.

Here, we report on the self-assembly at the solid/liquid interface of Pt(II) complex **Pt-Py-iCyt** (Scheme 1) into discrete supramolecular architectures held together *via* intermolecular hydrogen bonds between isocytosine moieties. In particular, we show the formation of polycrystalline structures composed of various polygonal assemblies including trimers, tetramers, pentamers and hexamers stabilized by distinct hydrogen bond pairing.

[a] Laboratoire de Nanochimie, ISIS & icFRC, Université de Strasbourg & CNRS, 8 allée Gaspard Monge, 67000 Strasbourg, France. E-mail: samori@unistra.fr

[b] Laboratoire de Chimie et des Biomatériaux Supramoléculaires, ISIS & icFRC, Université de Strasbourg & CNRS, 8 allée Gaspard Monge, 67000 Strasbourg, France

[c] Institute for Materials Sciences and Max Bergmann Center of Biomaterials, TU Dresden, 01062 Dresden, Germany

[d] Dresden Center for Computational Materials Science (DCCMS), TU Dresden, 01062 Dresden, Germany

[e] Center for Advancing Electronics Dresden, TU Dresden, 01062 Dresden, Germany. E-mail: projects@tu-dresden.de

† Electronic supplementary information (ESI) available: Experimental details, synthesis, and details of DFT calculations. See DOI: 10.1039/c6cc05087e

Scheme 1 Chemical structure of the Pt(II) complex (**Pt-Py-iCyt**). Hydrogen-bonding donor and acceptor sites are indicated in blue and red, respectively.

Supramolecular systems, where Pt(II) ions have been directly coordinated to nucleobases, have been the subject of numerous studies.[28–31] Certain platinum complexes of purine and pyrimidine derivatives were found to present promising properties as anti-tumor drugs.[32,33] Here we demonstrate for the first time that nucleobases, and in particular isocytosine, can be used to steer the 2D assembly of Pt(II) complexes through hydrogen bonding interactions between nucleobases. We support our experimental findings by performing density functional theory (DFT) calculations, and analysing both the strength of hydrogen bonding and the interactions with the graphite substrate. We also simulate the STM images to get an in depth understanding of the electronic features of the molecular architectures.

Initially, we investigated the self-assembly of **Py-iCyt** at the solid/liquid interface (see the ESI† for details). STM characterization revealed that **Py-iCyt** forms a supramolecular ribbon-like motif at the interface between the solution of **Py-iCyt** in 1-phenyloctane and highly oriented pyrolytic graphite (HOPG). Such a motif is in good agreement with previous observations on supramolecular structures of 6-methylisocytosine derivatives[34,35] and 6-[4-(octyloxy)phenyl]isocytosine.[36] This means that the functionalization of isocytosine with a pyridine unit does not influence its self-assembly behaviour at the solid/liquid interface.

We then extended our studies to the self-assembly of **Pt-Py-iCyt** at surfaces by applying a 4 µL drop of 100 ± 2 µM solution in 1-phenyloctane on a freshly cleaved HOPG substrate. The incorporation of the sterically demanding **CF$_3$-Pt** moiety in the scaffold led to a dramatic change in the self-assembly behaviour. The STM image in Fig. 1a displays discrete supramolecular cyclic architectures. All these cyclic assemblies have been identified and are portrayed in Fig. 1b: trimers (iC3, white), tetramers (iC4, blue), pentamers (iC5, green), half of hexamers (1/2iC6, red) and hexamers (iC6, yellow).

Statistical analysis of these experimentally observed cyclic arrangements was performed on ten independent STM experiments, also by exploring different regions of the samples. Fig. S9 in the ESI† summarizes the occurrence of each self-assembled discrete motif, which has been monitored and identified. Such an analysis revealed that two supramolecular species dominate, *i.e.* 1/2iC6 (45%)

and iC6 (35%), suggesting that they are both energetically favoured over the other cyclic motifs, *i.e.* iC5, iC4 and iC3 assemblies. The analysis of the number of monomers involved in various motifs further supports such an observation. Fig. S9 (ESI†) shows that >80% of the adsorbed molecules is being involved in the formation of either iC6 (50%) or 1/2iC6 (32%) structures.

The stability of the different supramolecular assemblies and their corresponding electronic structures was computed at the density functional theory (DFT) level with the standard implementation in the CP2K package.

We also simulated the STM images of ordered molecular motifs (iC6, iC5, iC4, iC3 and 1/2iC6) and the results are presented in Fig. 2 (right panel). A good agreement is found between the experimental and simulated STM images when the complex is packed onto graphite in iC6, iC5, iC4, iC3 and 1/2iC6 (Fig. 2). All molecular motifs randomly co-exist on the HOPG surface. iC6 and 1/2iC6, which are formed, respectively, by six and three **Pt-Py-iCyt**, are stabilized by hydrogen bonding
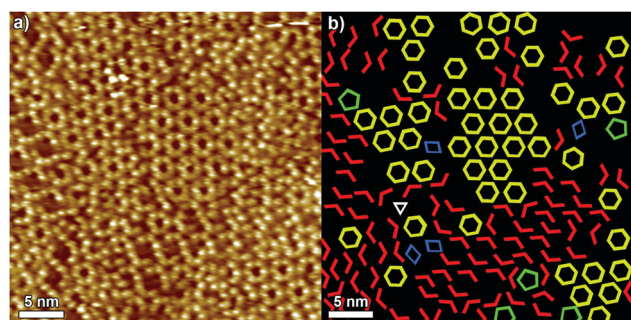

Fig. 1 (a) Height STM image of **Pt-Py-iCyt** at the solution/HOPG interface. Scanning tunnelling parameters: average tunnelling current (I_t) = 25 pA, tip bias voltage (V_t) = −450 mV. (b) Model of different self-assembled molecular motifs.
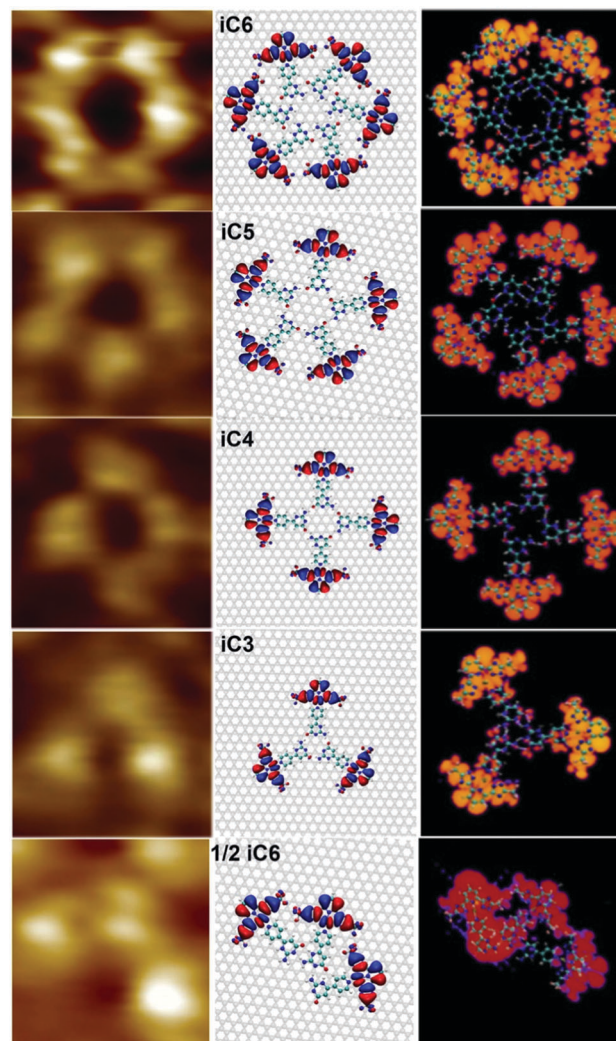

Fig. 2 (left) STM images of different **Pt-Py-iCyt** motifs. (middle) Simulated structures on graphene. (right) Simulated STM images of different motifs.

motifs of type O(3)···H–N(6) and N(4)···H–N(5), formed between isocytosine groups (Fig. 2). The self-assembly of the molecular architectures iC3, iC4 and iC5 can be explained by the formation of electrostatic interactions O(3)···H–N(6) occurring between the isocytosine groups of adjacent molecules. The different intermolecular interactions of the polygonal discrete architectures are explicitly illustrated in Fig. S15 in the ESI† as well as the self-assembly of the **Py-iCyt** ligand.

The relevant electronic structural features of the molecular building block (**Pt-Py-iCyt**) are illustrated in Fig. S14 in the ESI.† Panels b–d show the HOMO−1, HOMO and LUMO of the complex. The gap between the HOMO and HOMO−1 states was computed to be 45 meV. The LUMO level of **Pt-Py-iCyt** is spread over the molecular skeleton whereas the HOMO−1 is located only on the fluorinated part (**Pt-CF₃**). We also show the HOMO distribution of the different suggested molecular motifs as well as the ligand ribbons (Fig. S15, ESI†). The rather high localization degree of the HOMOs in the different motifs can be understood as follows: Pt has two free electrons, one in the d-level ($5d^9$) and one free electron in the s level ($6s^2$). Orbital localization is achieved by hybridization of the d free electron of Pt with the π orbitals generated by the ligand (four nitrogen atoms). Also, the four nitrogen atoms generate an effective crystal field splitting on Pt and therefore the d states jump to the upper part of the electronic structure and not the s state.

The interpretation of the molecular motifs monitored experimentally by STM is fully consistent with STM simulations. iC6 was generated through the formation of hydrogen bonds between isocytosine groups leading to a circular motif (Fig. 2). The observed contrast of different motifs – for example a dark center and a bright contour of iC6 (Fig. 2, right) – is due to HOMO levels of the assembled complexes. For this reason and because the STM images are recorded with a negative sample bias (occupied states), each individual **Pt-Py-iCyt** complex appears as a bright isolated protrusion in different molecular motifs. Three, four, five and six molecules are self-assembled to form, respectively, 1/2iC6 or iC3, iC4, iC5 and iC6 (details in the ESI†).

In order to investigate the mechanical stability of the different supramolecular motifs, we have calculated the dissociation energy for each suggested supramolecular structure shown in the middle panel of Fig. 2. We have defined the dissociation energy as:

$$E_{\text{diss}} = E_N - E_{N-1} - E_{\text{SM}} \tag{1}$$

where N is the number of molecular units within a given discrete supramolecular motif, E_N and E_{N-1} are the total energies of a given supramolecular motif containing N and $N − 1$ molecular units (monomers), respectively, and E_{SM} is the energy of a single isolated monomer. Energy E_{N-1} is computed by first removing a monomer from the supramolecular motif and subsequently performing a structural relaxation of the system.

Fig. 3 shows the computed dissociation energies of the molecular motifs. The number of hydrogen bonds, their nature and the degree of molecular packing play a crucial role in the dissociation energy of the molecular motifs. The highest dissociation energies were observed for iC6 and 1/2iC6 motifs, both
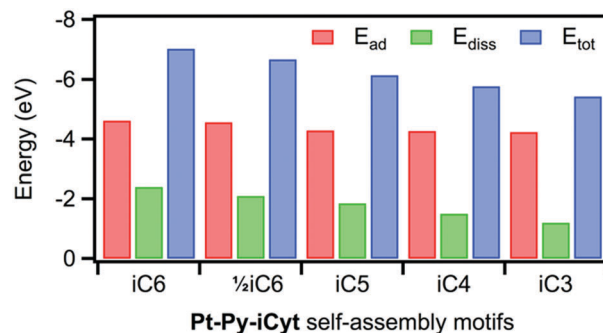

Fig. 3 Calculated adsorption (E_{ad}, red), dissociation (E_{diss}, green) and the total ($E_{\text{tot}} = E_{\text{ad}} + E_{\text{diss}}$, blue) energies of different molecular motifs self-assembled by **Pt-Py-iCyt** complex.

formed through O(3)···H–N(6) and N(4)···H–N(5) hydrogen bonding. Lower E_{diss} values have been observed for iC3–iC5 structures, which are stabilized via a weaker type of H-bonding, i.e. O(3)···H–N(6). The higher degree of molecular packing from iC3 to iC5 leads to a slight decrease of dissociation energies as a result of the repulsive interaction between the fluorine groups.

The optimized structures of the different supramolecular motifs on the graphene surface are shown in Fig. 2 (middle panel). The adsorption energies E_{ad} of these structures are reported in Fig. 3. Rather weak yet comparable interaction energies of **Pt-Py-iCyt** with the graphene substrate were found for all molecular structures (below 30 meV per atom). The STM analysis of films prepared from **Pt-Py-iCyt** solutions revealed the formation of polycrystalline structures dominated by iC6 and 1/2iC6 assemblies (ca. 80%; Fig. S9 in the ESI†), which is in good agreement with the results of the theoretical studies. In particular, both iC6 and 1/2iC6 assemblies are being favoured among all **Pt-Py-iCyt** structures, a finding, which can be directly correlated with the largest energies of dissociation. While the strength of intermolecular interactions plays a major role in the **Pt-Py-iCyt** self-assembly, the impact of the adsorption energies can be neglected, as E_{ad} were found to be comparable among all **Pt-Py-iCyt** assemblies.

In summary, we have performed STM study and DFT analysis on the formation of different polygonal discrete cyclic supramolecular motifs formed by the isocytosine based Pt(II) complex at the solution/HOPG interface through hydrogen bonding interactions between isocytosine groups of **Pt-Py-iCyt**. Both the experimental and the theoretical results provided unambiguous evidence that the formation of hexameric and half-hexameric motifs of **Pt-Py-iCyt** molecules is thermodynamically favoured, as ruled by the strength of the association energy. Nevertheless, pentamers, tetramers and trimers are also observed at the solid/liquid interface. The approach described in this work can be exploited to control the supramolecular structure of Pt(II) complexes at the surface, and consequently as a way for tuning the photophysical properties of such materials.

Notes and references

1 J. V. Barth, G. Costantini and K. Kern, *Nature*, 2005, **437**, 671–679.
2 M. Stöhr, M. Wahl, C. H. Galka, T. Riehm, T. A. Jung and L. H. Gade, *Angew. Chem., Int. Ed.*, 2005, **44**, 7394–7398.
3 J. A. A. W. Elemans, R. Van Hameren, R. J. M. Nolte and A. E. Rowan, *Adv. Mater.*, 2006, **18**, 1251–1266.
4 G. P. Spada, S. Lena, S. Masiero, S. Pieraccini, M. Surin and P. Samorì, *Adv. Mater.*, 2008, **20**, 2433–2438.
5 T. Kudernac, S. B. Lei, J. A. A. W. Elemans and S. De Feyter, *Chem. Soc. Rev.*, 2009, **38**, 402–421.
6 D. Bonifazi, S. Mohnani and A. Llanes-Pallas, *Chem. – Eur. J.*, 2009, **15**, 7004–7025.
7 J. A. G. Williams, *Photochemistry and Photophysics of Coordination Compounds II*, Springer, 2007, pp. 205–268.
8 C. A. Strassert, C. H. Chien, M. D. Galvez Lopez, D. Kourkoulos, D. Hertel, K. Meerholz and L. De Cola, *Angew. Chem., Int. Ed.*, 2011, **50**, 946–950.
9 N. K. Allampally, C. A. Strassert and L. De Cola, *Dalton Trans.*, 2012, **41**, 13132–13137.
10 V. M. Miskowski and V. H. Houlding, *Inorg. Chem.*, 1989, **28**, 1529–1533.
11 B. Ma, J. Li, P. I. Djurovich, M. Yousufuddin, R. Bau and M. E. Thompson, *J. Am. Chem. Soc.*, 2005, **127**, 28–29.
12 M. Mydlak, M. Mauro, F. Polo, M. Felicetti, J. Leonhardt, G. Diener, L. De Cola and C. A. Strassert, *Chem. Mater.*, 2011, **23**, 3659–3667.
13 M. Mauro, A. Aliprandi, D. Septiadi, N. S. Kehr and L. De Cola, *Chem. Soc. Rev.*, 2014, **43**, 4144–4166.
14 F. Rosei, M. Schunack, Y. Naitoh, P. Jiang, A. Gourdon, E. Laegsgaard, I. Stensgaard, C. Joachim and F. Besenbacher, *Prog. Surf. Sci.*, 2003, **71**, 95–146.
15 A. Nickel, R. Ohmann, J. Meyer, M. Grisolia, C. Joachim, F. Moresco and G. Cuniberti, *ACS Nano*, 2013, **7**, 191–197.
16 D. den Boer, M. Li, T. Habets, P. Iavicoli, A. E. Rowan, R. J. M. Nolte, S. Speller, D. B. Amabilino, S. De Feyter and J. A. A. W. Elemans, *Nat. Chem.*, 2013, **5**, 621–627.
17 S. Haq, F. Hanke, J. Sharp, M. Persson, D. B. Amabilino and R. Raval, *ACS Nano*, 2014, **8**, 8856–8870.
18 Y. Yu, J. Lin, Y. Wang, Q. Zeng and S. B. Lei, *Chem. Commun.*, 2016, **52**, 6609–6612.
19 M. Lackinger, S. Griessl, W. M. Heckl, M. Hietschold and G. W. Flynn, *Langmuir*, 2005, **21**, 4984–4988.
20 A. Llanes-Pallas, C.-A. Palma, L. Piot, A. Belbakra, A. Listorti, M. Prato, P. Samorì, N. Armaroli and D. Bonifazi, *J. Am. Chem. Soc.*, 2009, **131**, 509–520.
21 J. M. MacLeod, O. Ivasenko, C. Fu, T. Taerum, F. Rosei and D. F. Perepichka, *J. Am. Chem. Soc.*, 2009, **131**, 16844–16850.
22 O. Ivasenko and D. F. Perepichka, *Chem. Soc. Rev.*, 2011, **40**, 191–206.
23 M. El Garah, R. C. Perone, A. S. Bonilla, S. Haar, M. Campitiello, R. Gutierrez, G. Cuniberti, S. Masiero, A. Ciesielski and P. Samorì, *Chem. Commun.*, 2015, **51**, 11677–11680.
24 R. Otero, M. Schock, L. M. Molina, E. Laegsgaard, I. Stensgaard, B. Hammer and F. Besenbacher, *Angew. Chem., Int. Ed.*, 2005, **44**, 2270–2275.
25 W. Xu, R. E. A. Kelly, H. Gersen, E. Laegsgaard, I. Stensgaard, L. N. Kantorovich and F. Besenbacher, *Small*, 2009, **5**, 1952–1956.
26 L. K. Wang, H. H. Kong, C. Zhang, Q. Sun, L. L. Cai, Q. G. Tan, F. Besenbacher and W. Xu, *ACS Nano*, 2014, **8**, 11799–11805.
27 M. Cai, A. L. Marlow, J. C. Fettinger, D. Fabris, T. J. Haverlock, B. A. Moyer and J. T. Davis, *Angew. Chem., Int. Ed.*, 2000, **39**, 1283–1285.
28 B. T. Khan and S. M. Zakeeruddin, *Transition Met. Chem.*, 1991, **16**, 119–121.
29 H. Rauter, I. Mutikainen, M. Blomberg, C. J. L. Lock, P. AmoOchoa, E. Freisinger, L. Randaccio, E. Zangrando, E. Chiarparin and B. Lippert, *Angew. Chem., Int. Ed.*, 1997, **36**, 1296–1301.
30 D. Gupta, M. Huelsekopf, M. M. Cerda, R. Ludwig and B. Lippert, *Inorg. Chem.*, 2004, **43**, 3386–3393.
31 D. Gupta, M. Roitzsch and B. Lippert, *Chem. – Eur. J.*, 2005, **11**, 6643–6652.
32 A. G. Quiroga, *J. Inorg. Biochem.*, 2012, **114**, 106–112.
33 X. Wang, X. Wang and Z. Guo, *Acc. Chem. Res.*, 2015, **48**, 2622–2631.
34 L. M. Toledo, K. Musa, J. W. Lauher and F. W. Fowler, *Chem. Mater.*, 1995, **7**, 1639–1647.
35 P. R. Lowe, C. H. Schwalbe and G. J. B. Williams, *Acta Crystallogr., Sect. C: Cryst. Struct. Commun.*, 1987, **43**, 330–333.
36 A. Ciesielski, S. Colella, L. Zalewski, B. Bruchmann and P. Samorì, *CrystEngComm*, 2011, **13**, 5535–5537.